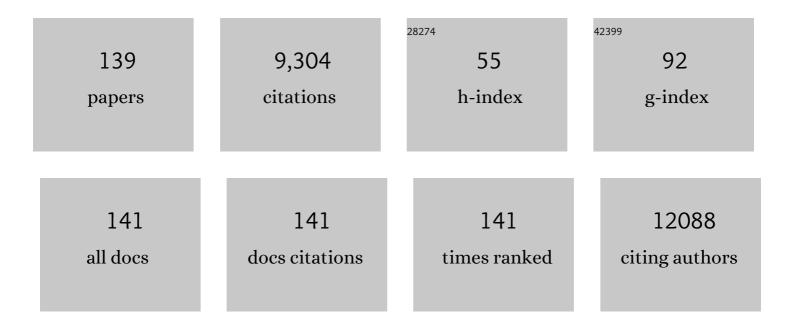
Xiaoxu Zhao

List of Publications by Year in descending order

Source: https://exaly.com/author-pdf/2272888/publications.pdf Version: 2024-02-01



#	Article	IF	CITATIONS
1	Hierarchically Porous Carbon Plates Derived from Wood as Bifunctional ORR/OER Electrodes. Advanced Materials, 2019, 31, e1900341.	21.0	320
2	Direct Synthesis of Largeâ€Area 2D Mo ₂ C on In Situ Grown Graphene. Advanced Materials, 2017, 29, 1700072.	21.0	305
3	Scalable two-step annealing method for preparing ultra-high-density single-atom catalyst libraries. Nature Nanotechnology, 2022, 17, 174-181.	31.5	279
4	Chemical Vapor Deposition of Large-Size Monolayer MoSe ₂ Crystals on Molten Glass. Journal of the American Chemical Society, 2017, 139, 1073-1076.	13.7	258
5	Chemically Exfoliated VSe ₂ Monolayers with Roomâ€Temperature Ferromagnetism. Advanced Materials, 2019, 31, e1903779.	21.0	251
6	Atomically-thin Bi2MoO6 nanosheets with vacancy pairs for improved photocatalytic CO2 reduction. Nano Energy, 2019, 61, 54-59.	16.0	243
7	Fabrication of Flexible Thermoelectric Thin Film Devices by Inkjet Printing. Small, 2014, 10, 3551-3554.	10.0	219
8	Defect Engineering of Two-Dimensional Transition-Metal Dichalcogenides: Applications, Challenges, and Opportunities. ACS Nano, 2021, 15, 2165-2181.	14.6	217
9	Phase Restructuring in Transition Metal Dichalcogenides for Highly Stable Energy Storage. ACS Nano, 2016, 10, 9208-9215.	14.6	216
10	Epitaxial Growth of Centimeter-Scale Single-Crystal MoS ₂ Monolayer on Au(111). ACS Nano, 2020, 14, 5036-5045.	14.6	211
11	Olivine-Type Nanosheets for Lithium Ion Battery Cathodes. ACS Nano, 2013, 7, 5637-5646.	14.6	210
12	Atomically Dispersed Cobalt Trifunctional Electrocatalysts with Tailored Coordination Environment for Flexible Rechargeable Zn–Air Battery and Selfâ€Đriven Water Splitting. Advanced Energy Materials, 2020, 10, 2002896.	19.5	210
13	Engineering covalently bonded 2D layered materials by self-intercalation. Nature, 2020, 581, 171-177.	27.8	185
14	Ultrasensitive 2D Bi ₂ O ₂ Se Phototransistors on Silicon Substrates. Advanced Materials, 2019, 31, e1804945.	21.0	183
15	Interface confined hydrogen evolution reaction in zero valent metal nanoparticles-intercalated molybdenum disulfide. Nature Communications, 2017, 8, 14548.	12.8	174
16	Chemical Stabilization of 1T′ Phase Transition Metal Dichalcogenides with Giant Optical Kerr Nonlinearity. Journal of the American Chemical Society, 2017, 139, 2504-2511.	13.7	171
17	Molecular Beam Epitaxy of Highly Crystalline Monolayer Molybdenum Disulfide on Hexagonal Boron Nitride. Journal of the American Chemical Society, 2017, 139, 9392-9400.	13.7	167
18	Molecular-Beam Epitaxy of Two-Dimensional In ₂ Se ₃ and Its Giant Electroresistance Switching in Ferroresistive Memory Junction. Nano Letters, 2018, 18, 6340-6346.	9.1	163

Хіаохи Zhao

#	Article	IF	CITATIONS
19	Highly Efficient 2D NIRâ€II Photothermal Agent with Fenton Catalytic Activity for Cancer Synergistic Photothermal–Chemodynamic Therapy. Advanced Science, 2020, 7, 1902576.	11.2	153
20	Single-Atom Coated Separator for Robust Lithium–Sulfur Batteries. ACS Applied Materials & Interfaces, 2019, 11, 25147-25154.	8.0	152
21	A non-dispersion strategy for large-scale production of ultra-high concentration graphene slurries in water. Nature Communications, 2018, 9, 76.	12.8	151
22	Atomic engineering of high-density isolated Co atoms on graphene with proximal-atom controlled reaction selectivity. Nature Communications, 2018, 9, 3197.	12.8	146
23	Gate-Tunable In-Plane Ferroelectricity in Few-Layer SnS. Nano Letters, 2019, 19, 5109-5117.	9.1	129
24	Chemical Vapor Deposition of Highâ€Quality Large‣ized MoS ₂ Crystals on Silicon Dioxide Substrates. Advanced Science, 2016, 3, 1500033.	11.2	128
25	<i>In Situ</i> Observation and Electrochemical Study of Encapsulated Sulfur Nanoparticles by MoS ₂ Flakes. Journal of the American Chemical Society, 2017, 139, 10133-10141.	13.7	126
26	Engineering Local and Global Structures of Single Co Atoms for a Superior Oxygen Reduction Reaction. ACS Catalysis, 2020, 10, 5862-5870.	11.2	126
27	Controllable deuteration of halogenated compounds by photocatalytic D2O splitting. Nature Communications, 2018, 9, 80.	12.8	123
28	Atomically Dispersed Indium Sites for Selective CO ₂ Electroreduction to Formic Acid. ACS Nano, 2021, 15, 5671-5678.	14.6	121
29	Phase-controllable growth of ultrathin 2D magnetic FeTe crystals. Nature Communications, 2020, 11, 3729.	12.8	120
30	Controlled Growth and Thicknessâ€Dependent Conductionâ€Type Transition of 2D Ferrimagnetic Cr ₂ S ₃ Semiconductors. Advanced Materials, 2020, 32, e1905896.	21.0	114
31	Controlled growth of ultrathin Mo ₂ C superconducting crystals on liquid Cu surface. 2D Materials, 2017, 4, 011012.	4.4	112
32	Atomically-precise dopant-controlled single cluster catalysis for electrochemical nitrogen reduction. Nature Communications, 2020, 11, 4389.	12.8	110
33	Mo-Terminated Edge Reconstructions in Nanoporous Molybdenum Disulfide Film. Nano Letters, 2018, 18, 482-490.	9.1	105
34	Printable two-dimensional superconducting monolayers. Nature Materials, 2021, 20, 181-187.	27.5	102
35	Enhanced Recyclability, Stability, and Selectivity of CdS/C@Fe ₃ O ₄ Nanoreactors for Orientation Photodegradation of Ciprofloxacin. Chemistry - A European Journal, 2015, 21, 18528-18533.	3.3	100
36	Rapid, Scalable Construction of Highly Crystalline Acylhydrazone Two-Dimensional Covalent Organic Frameworks via Dipole-Induced Antiparallel Stacking. Journal of the American Chemical Society, 2020, 142, 4932-4943.	13.7	99

#	Article	IF	CITATIONS
37	Tuning the Spin Density of Cobalt Single-Atom Catalysts for Efficient Oxygen Evolution. ACS Nano, 2021, 15, 7105-7113.	14.6	90
38	Partitioning the interlayer space of covalent organic frameworks by embedding pseudorotaxanes in their backbones. Nature Chemistry, 2020, 12, 1115-1122.	13.6	88
39	Ordered clustering of single atomic Te vacancies in atomically thin PtTe2 promotes hydrogen evolution catalysis. Nature Communications, 2021, 12, 2351.	12.8	83
40	Specific oriented recognition of a new stable ICTX@Mfa with retrievability for selective photocatalytic degrading of ciprofloxacin. Catalysis Science and Technology, 2016, 6, 1367-1377.	4.1	79
41	Single crystal of a one-dimensional metallo-covalent organic framework. Nature Communications, 2020, 11, 1434.	12.8	77
42	Photoluminescence Upconversion by Defects in Hexagonal Boron Nitride. Nano Letters, 2018, 18, 6898-6905.	9.1	76
43	Differentiating Polymorphs in Molybdenum Disulfide via Electron Microscopy. Advanced Materials, 2018, 30, e1802397.	21.0	75
44	Molecular Beam Epitaxy of Highly Crystalline MoSe ₂ on Hexagonal Boron Nitride. ACS Nano, 2018, 12, 7562-7570.	14.6	70
45	Enhanced Valley Zeeman Splitting in Fe-Doped Monolayer MoS ₂ . ACS Nano, 2020, 14, 4636-4645.	14.6	69
46	Atomâ€byâ€Atom Fabrication of Monolayer Molybdenum Membranes. Advanced Materials, 2018, 30, e1707281.	21.0	66
47	Improved photoelectric performance via fabricated heterojunction g-C3N4/TiO2/HNTs loaded photocatalysts for photodegradation of ciprofloxacin. Journal of Industrial and Engineering Chemistry, 2018, 64, 206-218.	5.8	66
48	A novel hollow capsule-like recyclable functional ZnO/C/Fe ₃ O ₄ endowed with three-dimensional oriented recognition ability for selectively photodegrading danofloxacin mesylate. Catalysis Science and Technology, 2016, 6, 6513-6524.	4.1	65
49	Temperature- and Phase-Dependent Phonon Renormalization in 1Tâ€2-MoS ₂ . ACS Nano, 2018, 12, 5051-5058.	14.6	63
50	Homoepitaxial Growth of Largeâ€ s cale Highly Organized Transition Metal Dichalcogenide Patterns. Advanced Materials, 2018, 30, 1704674.	21.0	63
51	Engineering and modifying two-dimensional materials by electron beams. MRS Bulletin, 2017, 42, 667-676.	3.5	62
52	Spin-Valley Locking Effect in Defect States of Monolayer MoS ₂ . Nano Letters, 2020, 20, 2129-2136.	9.1	61
53	Two-Dimensional Metallic NiTe ₂ with Ultrahigh Environmental Stability, Conductivity, and Electrocatalytic Activity. ACS Nano, 2020, 14, 9011-9020.	14.6	60
54	Lateral Epitaxy of Atomically Sharp WSe ₂ /WS ₂ Heterojunctions on Silicon Dioxide Substrates. Chemistry of Materials, 2016, 28, 7194-7197.	6.7	59

#	Article	IF	CITATIONS
55	Edge Segregated Polymorphism in 2D Molybdenum Carbide. Advanced Materials, 2019, 31, e1808343.	21.0	56
56	Zeroâ€Valent Palladium Singleâ€Atoms Catalysts Confined in Black Phosphorus for Efficient Semiâ€Hydrogenation. Advanced Materials, 2021, 33, e2008471.	21.0	55
57	Surface imprinting of a g-C ₃ N ₄ photocatalyst for enhanced photocatalytic activity and selectivity towards photodegradation of 2-mercaptobenzothiazole. RSC Advances, 2015, 5, 40726-40736.	3.6	54
58	Large Area Synthesis of 1Dâ€MoSe ₂ Using Molecular Beam Epitaxy. Advanced Materials, 2017, 29, 1605641.	21.0	54
59	High thermoelectric performance enabled by convergence of nested conduction bands in Pb7Bi4Se13 with low thermal conductivity. Nature Communications, 2021, 12, 4793.	12.8	53
60	Strain Modulation by van der Waals Coupling in Bilayer Transition Metal Dichalcogenide. ACS Nano, 2018, 12, 1940-1948.	14.6	51
61	Phaseâ€Controlled Synthesis of Monolayer Ternary Telluride with a Random Local Displacement of Tellurium Atoms. Advanced Materials, 2019, 31, e1900862.	21.0	51
62	From All-Triazine C ₃ N ₃ Framework to Nitrogen-Doped Carbon Nanotubes: Efficient and Durable Trifunctional Electrocatalysts. ACS Applied Nano Materials, 2019, 2, 7969-7977.	5.0	49
63	Two-Dimensional Metallic Vanadium Ditelluride as a High-Performance Electrode Material. ACS Nano, 2021, 15, 1858-1868.	14.6	49
64	High-Energy Gain Upconversion in Monolayer Tungsten Disulfide Photodetectors. Nano Letters, 2019, 19, 5595-5603.	9.1	41
65	Promoted Glycerol Oxidation Reaction in an Interface onfined Hierarchically Structured Catalyst. Advanced Materials, 2019, 31, e1804763.	21.0	40
66	Iron Single Atom Catalyzed Quinoline Synthesis. Advanced Materials, 2021, 33, e2101382.	21.0	39
67	Electronegativityâ€Induced Charge Balancing to Boost Stability and Activity of Amorphous Electrocatalysts. Advanced Materials, 2022, 34, e2100537.	21.0	39
68	Healing of Planar Defects in 2D Materials via Grain Boundary Sliding. Advanced Materials, 2019, 31, e1900237.	21.0	38
69	Visible-light driven room-temperature coupling of methane to ethane by atomically dispersed Au on WO3. Journal of Energy Chemistry, 2021, 61, 195-202.	12.9	38
70	A machine perspective of atomic defects in scanning transmission electron microscopy. InformaÄnÃ- Materiály, 2019, 1, 359-375.	17.3	37
71	Divergent Chemistry Paths for 3D and 1D Metalloâ€Covalent Organic Frameworks (COFs). Angewandte Chemie - International Edition, 2020, 59, 11527-11532.	13.8	35
72	MoTe ₂ : Semiconductor or Semimetal?. ACS Nano, 2021, 15, 12465-12474.	14.6	34

#	Article	IF	CITATIONS
73	Epitaxial growth of inch-scale single-crystal transition metal dichalcogenides through the patching of unidirectionally orientated ribbons. Nature Communications, 2022, 13, .	12.8	34
74	Biochemical evidence for a mitochondrial genetic modifier in the phenotypic manifestation of Leber's hereditary optic neuropathy-associated mitochondrial DNA mutation. Human Molecular Genetics, 2016, 25, 3613-3625.	2.9	32
75	Spaceâ€confined microwave synthesis of ternaryâ€layered BiOCl crystals with highâ€performance ultraviolet photodetection. InformaÄnÃ-Materiály, 2020, 2, 593-600.	17.3	32
76	Expedient synthesis of <i>E</i> -hydrazone esters and 1 <i>H</i> -indazole scaffolds through heterogeneous single-atom platinum catalysis. Science Advances, 2019, 5, eaay1537.	10.3	31
77	Progress and prospects of aberration-corrected STEM for functional materials. Ultramicroscopy, 2018, 194, 182-192.	1.9	29
78	High-Yield Exfoliation of Monolayer 1T'-MoTe ₂ as Saturable Absorber for Ultrafast Photonics. ACS Nano, 2021, 15, 18448-18457.	14.6	28
79	Ultralowâ€Threshold and Highâ€Quality Whisperingâ€Galleryâ€Mode Lasing from Colloidal Core/Hybridâ€Shell Quantum Wells. Advanced Materials, 2022, 34, e2108884.	21.0	28
80	Mutation analysis of Leber's hereditary optic neuropathy using a multi‑gene panel. Biomedical Reports, 2018, 8, 51-58.	2.0	27
81	The Atomic Circus: Small Electron Beams Spotlight Advanced Materials Down to the Atomic Scale. Advanced Materials, 2018, 30, e1802402.	21.0	27
82	Room Temperature Commensurate Charge Density Wave on Epitaxially Grown Bilayer 2H-Tantalum Sulfide on Hexagonal Boron Nitride. ACS Nano, 2020, 14, 3917-3926.	14.6	27
83	Building vertically-structured, high-performance electrodes by interlayer-confined reactions in accordion-like, chemically expanded graphite. Nano Energy, 2020, 70, 104482.	16.0	27
84	Controlled Growth of 3R Phase Tantalum Diselenide and Its Enhanced Superconductivity. Journal of the American Chemical Society, 2020, 142, 2948-2955.	13.7	27
85	High yield electrochemical exfoliation synthesis of tin selenide quantum dots for high-performance lithium-ion batteries. Journal of Materials Chemistry A, 2019, 7, 23958-23963.	10.3	26
86	New Family of Plasmonic Photocatalysts without Noble Metals. Chemistry of Materials, 2019, 31, 2320-2327.	6.7	25
87	Imprinting Ferromagnetism and Superconductivity in Single Atomic Layers of Molecular Superlattices. Advanced Materials, 2020, 32, e1907645.	21.0	25
88	2D Cairo Pentagonal PdPS: Air‧table Anisotropic Ternary Semiconductor with High Optoelectronic Performance. Advanced Functional Materials, 2022, 32, .	14.9	25
89	From Selfâ€Assembly Hierarchical hâ€BN Patterns to Centimeter‣cale Uniform Monolayer hâ€BN Film. Advanced Materials Interfaces, 2019, 6, 1801493.	3.7	23
90	Electrochemically Exfoliated Platinum Dichalcogenide Atomic Layers for High-Performance Air-Stable Infrared Photodetectors. ACS Applied Materials & Interfaces, 2021, 13, 8518-8527.	8.0	23

#	Article	IF	CITATIONS
91	Addressing the quantitative conversion bottleneck in single-atom catalysis. Nature Communications, 2022, 13, 2807.	12.8	23
92	Domain Engineering in ReS ₂ by Coupling Strain during Electrochemical Exfoliation. Advanced Functional Materials, 2020, 30, 2003057.	14.9	22
93	High-Concentration Niobium-Substituted WS2 Basal Domains with Reconfigured Electronic Band Structure for Hydrogen Evolution Reaction. ACS Applied Materials & Interfaces, 2019, 11, 34862-34868.	8.0	21
94	Growth of Si nanowires in porous carbon with enhanced cycling stability for Li-ion storage. Journal of Power Sources, 2014, 250, 160-165.	7.8	20
95	Hypertension-associated mitochondrial DNA 4401A>G mutation caused the aberrant processing of tRNAMet, all 8 tRNAs and ND6 mRNA in the light-strand transcript. Nucleic Acids Research, 2019, 47, 10340-10356.	14.5	20
96	Enhanced selective photocatalytic properties of a novel magnetic retrievable imprinted ZnFe ₂ O ₄ /PPy composite with specific recognition ability. RSC Advances, 2016, 6, 51877-51887.	3.6	19
97	Phaseâ€Controlled Synthesis of Monolayer W 1â^' x Re x S 2 Alloy with Improved Photoresponse Performance. Small, 2020, 16, 2000852.	10.0	18
98	Molecular engineered palladium single atom catalysts with an M-C ₁ N ₃ subunit for Suzuki coupling. Journal of Materials Chemistry A, 2021, 9, 11427-11432.	10.3	18
99	Phase-Tunable Synthesis and Etching-Free Transfer of Two-Dimensional Magnetic FeTe. ACS Nano, 2021, 15, 19089-19097.	14.6	18
100	Effects of precursor pre-treatment on the vapor deposition of WS ₂ monolayers. Nanoscale Advances, 2019, 1, 953-960.	4.6	17
101	Aqueous solution synthesis of (Sb, Bi)2(Te, Se)3 nanocrystals with controllable composition and morphology. Journal of Materials Chemistry C, 2013, 1, 6271.	5.5	16
102	Location-selective growth of two-dimensional metallic/semiconducting transition metal dichalcogenide heterostructures. Nanoscale, 2019, 11, 4183-4189.	5.6	16
103	Unveiling Atomic-Scale Moiré Features and Atomic Reconstructions in High-Angle Commensurately Twisted Transition Metal Dichalcogenide Homobilayers. Nano Letters, 2021, 21, 3262-3270.	9.1	15
104	Direct Laser Patterning of a 2D WSe ₂ Logic Circuit. Advanced Functional Materials, 2021, 31, 2009549.	14.9	15
105	Chemical Vapor Deposition of Superconducting FeTe _{1–<i>x</i>} Se _{<i>x</i>} Nanosheets. Nano Letters, 2021, 21, 5338-5344.	9.1	15
106	Synthesis of stable core–shell structured TiO ₂ @Fe ₃ O ₄ based on carbon derived from yeast with an enhanced photocatalytic ability. RSC Advances, 2016, 6, 46889-46899.	3.6	14
107	Few-layer 1T′ MoTe ₂ as gapless semimetal with thickness dependent carrier transport. 2D Materials, 2018, 5, 031010.	4.4	14
108	Fabrication of a visible-light In ₂ S ₃ /BiPO ₄ heterojunction with enhanced photocatalytic activity. New Journal of Chemistry, 2018, 42, 15136-15145.	2.8	13

Хіаохи Zhao

#	Article	IF	CITATIONS
109	Atomically Precise Single Metal Oxide Cluster Catalyst with Oxygenâ€Controlled Activity. Advanced Functional Materials, 2022, 32, .	14.9	13
110	Strong Moiré Excitons in High-Angle Twisted Transition Metal Dichalcogenide Homobilayers with Robust Commensuration. Nano Letters, 2022, 22, 203-210.	9.1	12
111	Controllable Synthesis Quadratic-Dependent Unsaturated Magnetoresistance of Two-Dimensional Nonlayered Fe ₇ S ₈ with Robust Environmental Stability. ACS Nano, 2022, 16, 8301-8308.	14.6	12
112	Model updating of suspended-dome using artificial neural networks. Advances in Structural Engineering, 2017, 20, 1727-1743.	2.4	11
113	Anisotropic point defects in rhenium diselenide monolayers. IScience, 2021, 24, 103456.	4.1	11
114	Divergent Chemistry Paths for 3D and 1D Metalloâ€Covalent Organic Frameworks (COFs). Angewandte Chemie, 2020, 132, 11624-11629.	2.0	10
115	An Anomalous Magneto-Optic Effect in Epitaxial Indium Selenide Layers. Nano Letters, 2020, 20, 5330-5338.	9.1	10
116	Learning motifs and their hierarchies in atomic resolution microscopy. Science Advances, 2022, 8, eabk1005.	10.3	10
117	A novel CdS photocatalyst based on magnetic fly ash cenospheres as the carrier: performance and mechanism. RSC Advances, 2014, 4, 60148-60157.	3.6	9
118	2D Electrolytes: Theory, Modeling, Synthesis, and Characterization. Advanced Materials, 2021, 33, 2100442.	21.0	9
119	Epitaxial Growth of Stepâ€Like Cr ₂ S ₃ Lateral Homojunctions Towards Versatile Conduction Polarities and Enhanced Transistor Performances. Small, 2022, 18, e2105744.	10.0	9
120	Overexpression of human mitochondrial alanyl-tRNA synthetase suppresses biochemical defects of the mt-tRNA ^{Ala} mutation in cybrids. International Journal of Biological Sciences, 2018, 14, 1437-1444.	6.4	8
121	Phenotype, genotype and long-term prognosis of 40 Chinese patients with isobutyryl-CoA dehydrogenase deficiency and a review of variant spectra in ACAD8. Orphanet Journal of Rare Diseases, 2021, 16, 392.	2.7	8
122	Chemical Vapor Deposition of Phaseâ€Pure 2D 1T rS ₂ . Physica Status Solidi - Rapid Research Letters, 2022, 16, .	2.4	8
123	Synthesis of Fe ₃ O ₄ /C with Cauliflower-Like BiVO ₄ for Improved Separation Efficiency of Charge Carriers and Photocatalytic Activity. Journal of Nanoscience and Nanotechnology, 2018, 18, 4675-4683.	0.9	7
124	Self-sacrificing template strategy to non-noble Bi modified BiVO4 for promoted visible light photocatalytic performance. Chemical Physics Letters, 2020, 755, 137786.	2.6	7
125	Nanocrystalline diamond film grown by pulsed linear antenna microwave CVD. Diamond and Related Materials, 2021, 119, 108576.	3.9	6
126	Electron beam triggered single-atom dynamics in two-dimensional materials. Journal of Physics Condensed Matter, 2021, 33, 063001.	1.8	6

#	ARTICLE	IF	CITATIONS
127	Solid-Ionic Memory in a van der Waals Heterostructure. ACS Nano, 2022, 16, 221-231.	14.6	6
128	Dimensional crossover in self-intercalated antiferromagnetic <mml:math xmlns:mml="http://www.w3.org/1998/Math/MathML"><mml:mrow><mml:msub><mml:mi mathvariant="normal">V<mml:mn>5</mml:mn></mml:mi </mml:msub><mml:msub><mml:mi mathvariant="normal">S<mml:mn>8</mml:mn></mml:mi </mml:msub></mml:mrow> nanoflakes. Physical Review B, 2022, 105, .</mml:math 	3.2	6
129	Thermal-Assisted Vertical Electron Injections in Few-Layer Pyramidal-Structured MoS ₂ Crystals. Journal of Physical Chemistry Letters, 2019, 10, 1292-1299.	4.6	5
130	A comparison of free-hand method and electromagnetic navigation technique for the distal locking during intramedullary nailing procedures: a meta-analysis. Archives of Orthopaedic and Trauma Surgery, 2021, 141, 45-53.	2.4	5
131	Singleâ€Atom Catalysts: Atomically Dispersed Cobalt Trifunctional Electrocatalysts with Tailored Coordination Environment for Flexible Rechargeable Zn–Air Battery and Selfâ€Driven Water Splitting (Adv. Energy Mater. 48/2020). Advanced Energy Materials, 2020, 10, 2070195.	19.5	4
132	Recent Developments in Chemical Vapor Deposition of 2D Magnetic Transition Metal Chalcogenides. ACS Applied Electronic Materials, 2022, 4, 3303-3324.	4.3	4
133	Lithography-free, high-density MoTe2 nanoribbon arrays. Materials Today, 2022, 58, 8-17.	14.2	4
134	Molybdenum Disulfid: Differentiating Polymorphs in Molybdenum Disulfide via Electron Microscopy (Adv. Mater. 47/2018). Advanced Materials, 2018, 30, 1870360.	21.0	2
135	Designing Energy Materials via Atomic-resolution Microscopy and Spectroscopy. Microscopy and Microanalysis, 2019, 25, 1998-1999.	0.4	1
136	Ultralowâ€Threshold and Highâ€Quality Whisperingâ€Galleryâ€Mode Lasing from Colloidal Core/Hybridâ€Shell Quantum Wells (Adv. Mater. 13/2022). Advanced Materials, 2022, 34, .	21.0	1
137	Frontispiece: Enhanced Recyclability, Stability, and Selectivity of CdS/C@Fe ₃ O ₄ Nanoreactors for Orientation Photodegradation of Ciprofloxacin. Chemistry - A European Journal, 2015, 21, .	3.3	0
138	Engineering and Modifying Two-Dimensional Materials via Electron Beams. Microscopy and Microanalysis, 2019, 25, 1474-1475.	0.4	0
139	Imaging and modifying 2D materials by STEM. , 2021, , .		0